Building Simulation 2003

Eighth International IBPSA Conference
Eindhoven, Netherlands
August 11-14, 2003

COMPUTER SIMULATION OF SOLAR RADIATION RECEIVED BY CURVED ROOF IN HOT-ARID REGIONS

Ahmed A. B. ELSERAGY[1], and Mohamed B. GADI[2]
[1] Ph.D. Researcher, School of The Built Environment, The University of Nottingham, UK
laxabee@nottingham.ac.uk, +44 (0) 115 84 66041
[2] Lecturer, School of The Built Environment, The University of Nottingham, UK
mohamed.gadi@nottingham.ac.uk, +44 (0) 115 9513118

ABSTRACT

This paper is part of continuing research aimed at exploring the relationship between the amount of solar radiation received by a curved roof and its geometrical configurations. It seeks better understanding of the solar performance of traditional curved roofs to be well integrated into buildings in developing countries, mainly in hot regions Fig. (1). A number of investigations has been carried out on curved roofs with varying cross-section ratios and orientations to study their solar radiation performances. This paper discusses the variations in Total Hourly Clear Sky Irradiance $\boldsymbol{I}_{(HTSC)}$ W/m^2 received by a semicircular curved roof and a flat roof. The geographical latitude of Aswan (23.58^{o}N) has been chosen to represent the hot regions of southern Egypt.

Fig. (1): Traditional Domes and Vaults

INTRODUCTION

Roof is the building-envelope element that is most exposed to the sun. It receives the highest amount of solar radiation, which is the main cause of summer overheating in hot-arid climates. In addition, to other climatic and physical factors, indoor thermal comfort in hot climates significantly depends on the reduction of the intensity of solar irradiance received by roofs in hot climates. Building form and specifically the roof plays an important role in keeping indoor environment thermally comfortable for occupants throughout the year without the use of artificial or mechanical devices. Therefore, roof form should follow number of insolation parameters in terms of controlling the quantity of received solar radiation on roof surface and enhance its thermal performance.

In this context, the paper aims to investigate the solar performance of vaulted roofs, which traditionally provided indoor thermal comfort. Prior to computer simulation, a number of equations and mathematical calculations verified that solar radiation received by a surface differs significantly according to its tilt angle from the horizontal and its orientation. Therefore, at the same geographical latitude, $\boldsymbol{I}_{(HTCS)}$ on surfaces remarkably varies according to their forms. The paper reviews the results of a computational investigation that has been carried out to calculate the $\boldsymbol{I}_{(HTCS)}$ on horizontal and tilted surfaces, which geometrically resemble the form of curved roofs. The computer simulation enables to run rapid and infinite calculations for large number of curved roofs with varying curvatures and orientations.

CURVED ROOF GEOMETRICAL RESEMBLANCE

For curved roofs, the proposed geometrical resemblance methodology in this paper is neither new nor only employed in this research work. Customary in CAD tools, most of curvy forms have been geometrically resembled by group of planar segments, pixels, or stripes. This technique is employed in most two and three-dimensional CAD drawings, Fig. (2). Sensibly, and regardless to the tested curvy form nature, the more resembling planar segments or pixels the more accurate results will be.

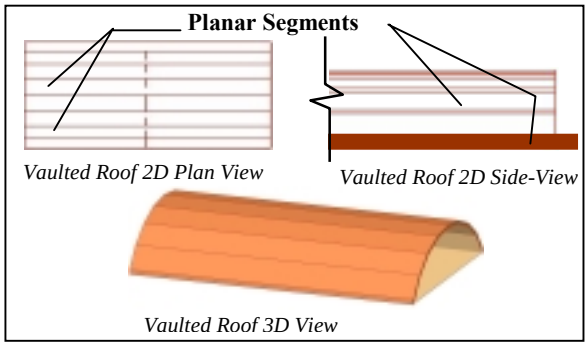

Fig. (2): CAD Drawings For Curved Forms

Fig. (3) shows a curved roof-cross section *(CCS)*, which has been geometrically resembled by two types of planar segments. This simplifies the calculations of solar radiation intensity on curved roof surfaces.

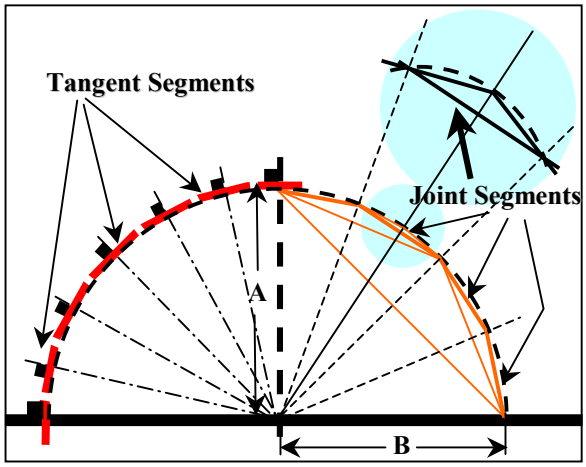

Fig. (3): The Two Proposed Planar Segments

According to their workability, tangent planar segments have been only used in the semicircular curved roof, which is discussed in this paper, Fig. (4). This is called the standard curved roof cross section $CCS_{(std)}$, in which A equals B. A number of CCSR with varuing curvatures, where A not always equal B *(i.e. A=B, A>B, & A<B)*, has been carried out in order to investigate the influence of the CCSR on the received solar radiation the intensity on curved roofs[1]. CCSR, where A does not equal B *(ellipse cases)*, must be resembled by joint-planar-segments, Fig. (4).

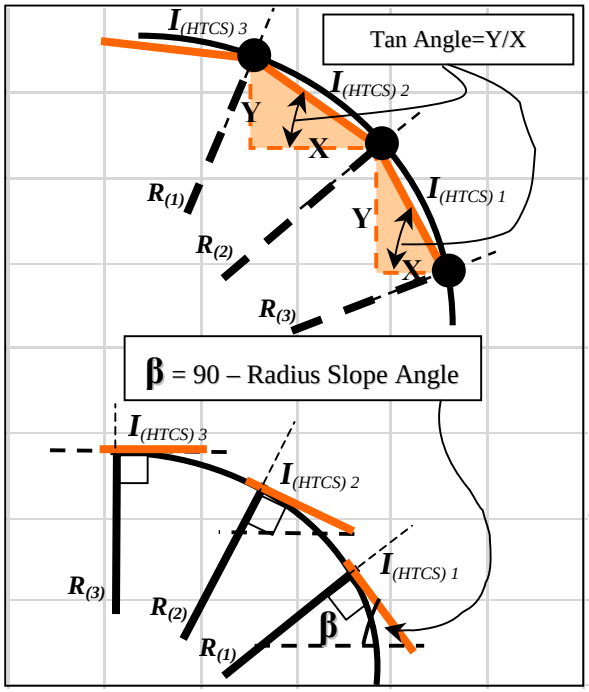

Fig. (4): Segments Slopes Within The Two Employed Planar Segments Methodologies

[1] The results of the differen curvatures CCSR are not included in this paper.

The gradients of both planar segments types can be geometrically and mathematically defined, Fig. (5) & Table (1).

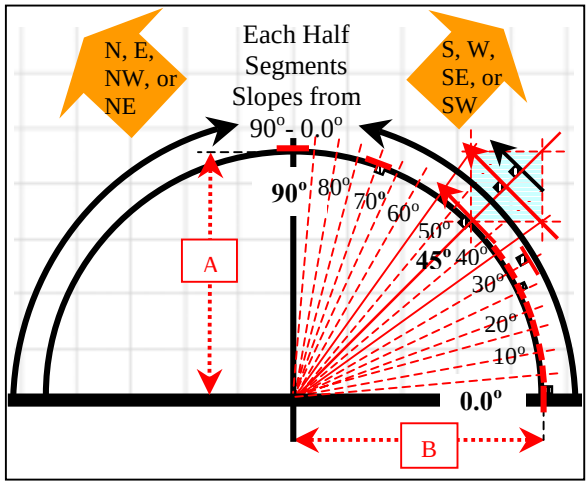

Fig. (5): The Geometrical Resemblance of The $CCS_{(std)}$ & Planar Segments Slopes

Table 1:Generated Segments Slopes

Radius Slopes *(Radian = 5°)* & Slope Angles of Resembling Planar Segments								
5°	**10°**	**15°**	**20°**	**25°**	**30°**	**35°**	**40°**	**45°**
85	80	75	70	65	60	55	50	45
50°	**55°**	**60°**	**65°**	**70°**	**75°**	**80°**	**85°**	**90°**
40	35	30	25	20	15	10	5	0.0

SIMULATION DESIGN AND TOOL

The paper compares between the Hourly Total Clear Sky Irradiance $I_{(HTCS)}$ on $CCS_{(std)}$, and flat roof. The geometrical resemblance of $CCS_{(std)}$ has been explained before in Fig. (4) & (5). $CCS_{(std)}$ has been geometrically resembled by 37 tangent segments. Each half of $CCS_{(std)}$ has been divided into eighteen tangent segments. The hourly clear sky irradiance $I_{(HTCS)}$ on the full CCS can be determined by calculating the average of the received $I_{(HTCS)}$ on number of planar segments along the $CCS_{(std)}$, equation (1).

$$I_{(HTCS)} = \frac{\sum (I_{(HTCS)}\,1 : I_{(HTCS)}\,37)}{37} \qquad (1)$$

The calculated average of the received $I_{(HTCS)}$ on full CCS or on selected part is valid and appropriate to compare between intensities (W/m^2) on different forms. While, for the calculations of the received $I_{(HTCS)}$ on an entire surface area of a form, the resulted average intensity W/m^2 has to be multiplied by this area (m^2). On the other hand, to compare between the total solar radiation intensities fall on two surface areas of two different forms, the surface areas have to be equal. In the case of different surface areas, the intensity W/m^2 has to be multiplied by a factor that represents the surface areas ratio.

Solar Radiation Simulation Model (SRSM) is a computer algorithm, which is developed by Professor R. H. B. Exell, 1999, King Mongkut's University of Technology Thonburi. The parametrical study in this paper is mainly based on the ***SRSM.*** It can be generally applied for the calculation of direct, diffuse, and ground reflected hourly irradiance on a surface at any orientation and slope according to the selected parameters and data inputs.

In general, the calculations methodology depends on computing the received $\boldsymbol{I}_{(HTCS)}$ on each tilted planar segment by the ***SRSM***, then calculating the average of the received $\boldsymbol{I}_{(HTCS)}$ on group of planar segments, which resemble either full CCS or a particular sector of a curved roof. Roof surface has to be defined geometrically in term of angles that determine both surface slope angle and azimuth angle *(orientation or the direction that the surface faces).*

DISCUSSION AND RESULTS ANALYSIS

$CCS_{(std)}$ Curvature Faces North & South

This is the first principal-orientation that the study will employ. In this case, the longitudinal axis *(perpendicular on the CCS)* is the East-West axis. The two halves of $CCS_{(std)}$ face northward and southward. This case will be tested repeatedly during summer and winter to point out in which season the curved roof can significantly reduce the received solar radiation than flat roofs.

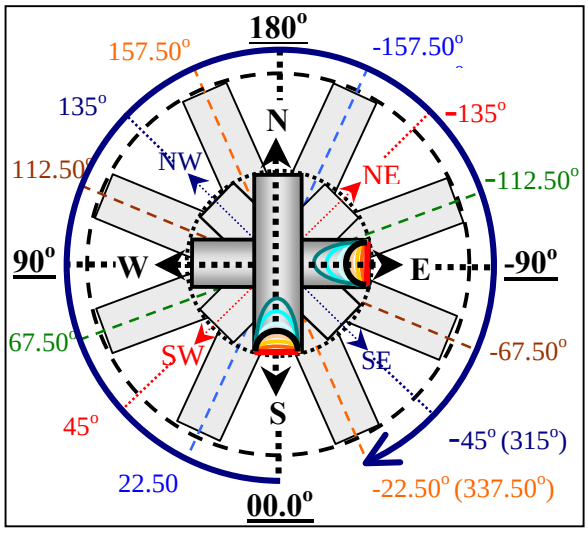

Fig. 6: Curved Roofs Orientations
($CCS_{(std)}$ Curvature Faces Principle-Directions)

$CCS_{(std)}$ Faces (N-S) During June

Fig. (7) shows the $\boldsymbol{I}_{(HTSC)}$ on flat and curved roof $CCS_{(std)}$ during summer. The maximum received solar radiation in both roofs take place at midday. At summer, $\boldsymbol{I}_{(HTSC)}$-curves *($\boldsymbol{I}_{(HTCS)}$-values distribution forms)* at both tested geometries $CCS_{(std)}$ and flat roof have similar characteristics.

Each roof $\boldsymbol{I}_{(HTCS)}$- curve ascends differently after 6:00 in the morning where both $\boldsymbol{I}_{(HTCS)}$-curves are still encountered. They reach their maximum at 12:00. During the afternoon solar radiation intensity on both roofs geometries descend differently till the two curves encounter each other again at 18:00, Fig. (7).

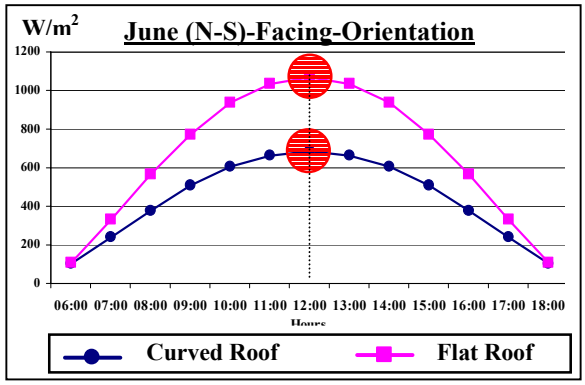

Fig. 7: $\boldsymbol{I}_{(HTCS)}$ (W/m^2) on Flat Roof and $CCS_{(std)}$

In both geometries ($CCS_{(std)}$ & flat roof), $\boldsymbol{I}_{(HTSC)}$-curve has symmetrical increase and decrease gradients around midday, Fig. (7). Approximately, at 6:00 and 18:00 both $CCS_{(std)}$ and flat roof receive equal $\boldsymbol{I}_{(HTSC)}$-values, 104 W/m^2 and 106W/m^2 respectively. The minimum difference between the two $\boldsymbol{I}_{(HTSC)}$-curves has been recorded at the early-morning and the late-afternoon. It slightly increases till it reaches the maximum at 12:00 *($1070 - 683 = 387\ W/m^2$)*. $\boldsymbol{I}_{(HTSC)}$-curve for flat roof starts and ends with steeper gradients comparatively to $CCS_{(std)}$ ones, then it gets smoother around 12:00 at both roofs geometries.

$CCS_{(std)}$ Faces (N-S) During December

Fig. (8) shows the $\boldsymbol{I}_{(HTSC)}$ on flat and curved roofs $CCS_{(std)}$ during winter. Identical to the previous scenario in summer, the maximum received solar radiation by each roof takes place at 12:00. Moreover, in winter both geometries $CCS_{(std)}$ and flat roof have similar characteristics of $\boldsymbol{I}_{(HTSC)}$-curves.

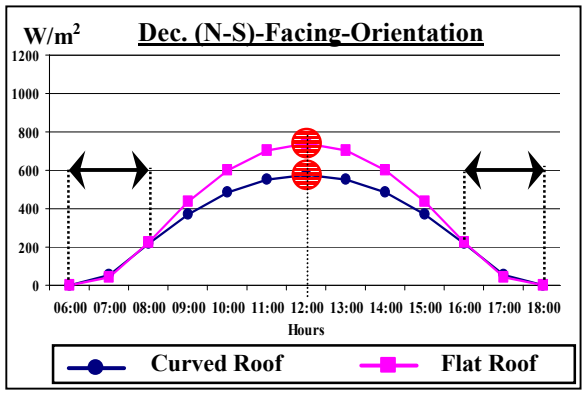

Fig. 8: $\boldsymbol{I}_{(HTCS)}$ (W/m^2) on Flat Roof and $CCS_{(std)}$

Each $I_{(HTCS)}$-curve ascends after 6:00 in the morning where both $I_{(HTCS)}$-curves are still encountered. They behave differently during 7:00. The two curves get very close during 8:00 before reaching their maximum at midday. During the afternoon period $I_{(HTCS)}$-curve for each roof geometry behaves symmetrical to its behaviour prior to 12:00. Each $I_{(HTCS)}$-curve descends differently till the two curves get very close again at 16:00 and they encounter each other at 18:00, Fig. (8).

In both geometries ($CCS_{(std)}$ & flat roof), $I_{(HTCS)}$-curve has symmetrical increase and decrease gradients in noon period. Moreover, $I_{(HTCS)}$-mirrored-values around midday, which both roofs geometries received are equal. $CCS_{(std)}$ receives slightly more solar radiation than the flat roof at 7:00 and 17:00, 55.5 W/m^2 and 40 W/m^2 respectively.

At 8:00 and 16:00, a similar scenario to what has been observed at 6:00 and 18:00 during summer, in which approximately equal $I_{(HTCS)}$-values are recorded at both $CCS_{(std)}$ and flat roof, 221 W/m^2 and 224 W/m^2 respectively. On the contrary to what has been observed in summer, the noticeable difference has been shifted 2 hours *(from 7:00 & 17:00 in summer to 9:00 & 15:00 in winter)*.

As shown previously in Fig. (8), the difference between the two geometries $I_{(HTCS)}$-curves records its minimum at the early-morning and the late-afternoon hours. It increases and reaches the maximum at 12:00 *(740 – 576 = 164 W/m^2)*. $I_{(HTCS)}$-curve for flat roof starts and ends with steeper gradients comparatively to $CCS_{(std)}$ ones It gets smoother around 12:00 at both geometries.

Fig. (8) also shows that during the early-morning and the late-afternoon hours $CCS_{(std)}$ and flat roof receive very close $I_{(HTCS)}$-values (nearly equal), which is dissimilar to (N-S) orientation in summer. This could be even better during winter in which there is no need to reduce the received solar radiation by roofs surfaces. Moreover, receiving solar radiation in winter at the early-morning and the late-afternoon hours is desirable.

$CCS_{(std)}$ Curvature Faces East & West

This is the second principal-orientation that the study will employ. In this case, the longitudinal axis *(perpendicular on the CCS)* is the (N-S) axis. The two halves of $CCS_{(std)}$ face eastward and westward. As it has been applied before in the previous principle-orientation, this case will be also tested independently during summer and winter. This determines the performance of curved roof in different seasons throughout the year.

$CCS_{(std)}$ Faces (E-W) During June

Fig. (9) shows the distribution forms of $I_{(HTCS)}$ received by flat and curved roof $CCS_{(std)}$ during summer. Similar to the case of summer while the two geometries face north and south, the maximum received solar radiation on both roofs at this orientation takes place at midday. Both tested-geometries $CCS_{(std)}$ and flat roof have similar characteristics of $I_{(HTCS)}$-curves, which ascend differently at each roof geometry after 6:00 in the morning where both curves are still countered. Both $I_{(HTCS)}$-curves get very close during 8:00 and before reaching their maximum at 12:00. During the afternoon $I_{(HTCS)}$-curves for each roof descends differently till the two curves get very close again at 17:00. They get countered at 18:00, Fig. (9).

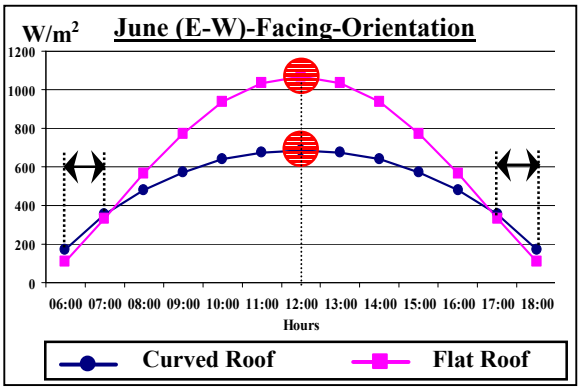

Fig. 9: $I_{(HTCS)}$ (W/m^2) on Flat Roof and $CCS_{(std)}$

$I_{(HTCS)}$-curves in both geometries ($CCS_{(std)}$ & flat roof) have symmetrical increases and decreases gradients around 12:00. Dissimilarly, at 6:00 and 18:00 both $CCS_{(std)}$ and flat roof do not receive equal $I_{(HTCS)}$-values, 170 W/m^2 and 106W/m^2 respectively. As shown in Fig. (9), the desirable difference between the two $I_{(HTCS)}$-curves records its minimum at 8:00 and 16:00. It slightly increases till it reaches the maximum at 12:00 *(1070 – 684 = 386 W/m^2)*, which is nearly identical to what has been recorded at (N-S) in summer. Flat roof $I_{(HTCS)}$-curve starts and ends with steeper gradients comparatively to $CCS_{(std)}$ ones. The gradients of both roofs $I_{(HTCS)}$-curves get smoother around 12:00.

Fig. (9) shows that throughout the day there are two time periods *(6:00-7:00 and 17:00-18:00)* in which $CCS_{(std)}$ receives more $I_{(HTCS)}$ than the flat roof. These time periods did not exist when the $CCS_{(std)}$ faced (N-S) in summer. The desirable time in which $CCS_{(std)}$ receives less $I_{(HTCS)}$ comparatively to flat roof is shorter 2 hours at (E-W) with the comparison to (N-S) in summer. For $CCS_{(std)}$ faces (E-W), this time period starts one hour later and it ends one hour earlier in comparison to (N-S).

$CCS_{(std)}$ Faces (E-W) During December

Fig. (10) shows the $I_{(HTCS)}$ on flat and curved roof during winter. Similar to all previous cases and particularly to the (N-S)-facing-orientation in winter, the maximum received solar radiation on both roofs takes place at midday. Moreover, both geometries $CCS_{(std)}$ and flat roof have similar characteristics for their $I_{(HTCS)}$-curves. Independently, each geometry $I_{(HTCS)}$-curve ascends after 6:00 in the morning where both $I_{(HTCS)}$-curves are still encountered. They behave differently during 7:00. The two curves get very close during 8:00 before reaching their maximum at midday as same as previous cases and scenarios. During the afternoon $I_{(HTCS)}$-curve of each geometry behaves symmetrically to its behaviour prior to 12:00. Each $I_{(HTCS)}$-curve descends differently till the two curves get very close again at 16:00. They encounter each other at 18:00, Fig. (10).

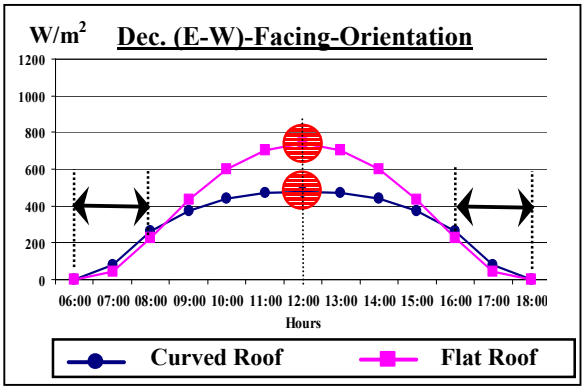

Fig. 10: $I_{(HTCS)}$ (W/m^2) on Flat Roof and $CCS_{(std)}$

In both geometries ($CCS_{(std)}$ & flat roof), $I_{(HTCS)}$ has symmetrical increase and decrease gradients around noon period. According to the low altitude angle of sun during winter, especially at sunrise and sunset, both $CCS_{(std)}$ and flat roof do not receive solar radiation at 6:00 in the morning and at 18:00 in the afternoon. Whereas, at 7:00 and 17:00 $CCS_{(std)}$ receives slightly more solar radiation than the flat roof, 55.5W/m² and 40W/m² respectively.

Both $CCS_{(std)}$ and flat roof receive 221W/m² and 224W/m² respectively in winter. Comparatively to summer of this orientation, the noticeable difference between the two roofs $I_{(HTCS)}$-values is shorter 2 hours. It is delayed one hour before 12:00 *(9:00 in winter instead of 8:00 in summer)*. While, this difference is recorded one hour earlier during the afternoon *(15:00 in winter instead of 16:00 in summer)*.

As shown in Fig. (9), the difference between the two $I_{(HTCS)}$-curves records its minimum at the early-morning and the late-afternoon hours. This difference increases and reaches the maximum at 12:00 *(740 – 576 = 164 W/m^2)*. Flat roof $I_{(HTCS)}$-curve starts and ends with steeper gradients comparatively to $CCS_{(std)}$ ones. Both roofs $I_{(HTCS)}$-curves get smoother around noon period.

Similar to what has been noticed previously during winter in (N-S)-facing-orientation, Fig. (10) also shows that during the early-morning and the late-afternoon hours $CCS_{(std)}$ receives more solar radiation than the received by the flat roof *(nearly very close values)*. Even more, the received solar radiation intensity by $CCS_{(std)}$ at (E-W) is slightly higher than that received by a similar geometry faces (N-S). This may add more credits for curved roof faces (E-W) in terms of receiving more solar radiation during winter.

$CCS_{(std)}$ Curvature Faces Northwest & Southeast

This is the first secondary-orientation that the study employs. In this case, the longitudinal axis *(perpendicular on the CCS)* is the (NE-SW) axis. The two halves of $CCS_{(std)}$ face NW and SE, Fig. (11). This case will be tested independently during summer and winter to clarify in which time of the year can curved roofs significantly receive less solar radiation with comparison to the flat roof.

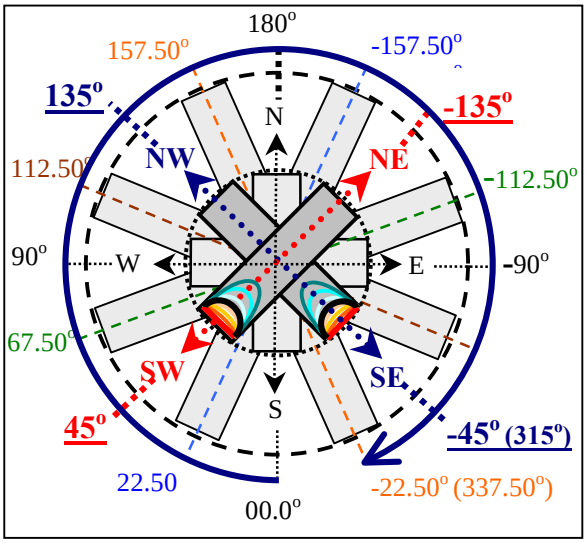

Fig. 11: Curved Roofs Orientations
($CCS_{(std)}$ Curvature Faces Secondary-Directions)

$CCS_{(std)}$ Faces (NW-SE) During June

Fig. (12) shows the $I_{(HTCS)}$ on flat and curved roof $CCS_{(std)}$ during summer. Similar to what has been discussed previously in the principal-directions applications, the maximum received solar radiation on both roofs also takes place at midday in this secondary-direction (NW-SE). According to its geometry, the $I_{(HTCS)}$-values on flat roof are not influenced by orientation. Therefore, they have symmetrical distribution form around the midday axis at any direction.

On the contrary, and due to its form elevation, $I_{(HTCS)}$-values *on* curved roof are significantly effected by $CCS_{(std)}$ orientation. Therefore, their distribution form is unsymmetrical around midday. Moreover, $I_{(HTCS)}$-mirrored-values around 12:00 are not equal. Independently, $I_{(HTCS)}$-curves in both geometries ascend after 6:00 in the morning where both are still encountered. They reach their maximum at midday. During the late-afternoon each geometry $I_{(HTCS)}$-curve descends differently till the two curves encounter each other again at 17:00. At 18:00 the two curves counter each other, Fig. (12).

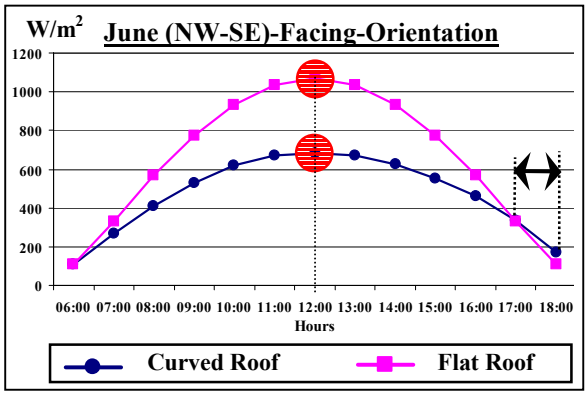

Fig. 12: $I_{(HTCS)}$ (W/m^2) on Flat Roof and $CCS_{(std)}$

$I_{(HTCS)}$-curves before midday in summer when $CCS_{(std)}$ faces (NW-SE) are very similar to (N-S)-principle-direction, whereas during afternoon both curves are similar to (E-W). $I_{(HTCS)}$-curve has similar increase and decrease gradients around noon period. During the afternoon $CCS_{(std)}$ $I_{(HTCS)}$-curve does not exactly display the same gradients as before 12:00.

Both geometries ($CCS_{(std)}$ & flat roof) receive approximately equal $I_{(HTCS)}$-values only at 6:00 in the morning, 108 W/m^2 and 106W/m^2 respectively, whereas they record 168 W/m^2 and 106 W/m^2 at 18:00. This was not the case during principle-directions, where $I_{(HTCS)}$-mirrored-values around the midday axis are equal . Consequently, the desirable difference between the two roofs $I_{(HTCS)}$-curves forms an unsymmetrical shape, Fig. (12).

As shown in Fig. (12) minimum difference is recorded at 6:00 and 17:00 instead of 6:00 and 18:00 as in (N-S) orientation. It slightly increases till it reaches the maximum at 12:00 *(1070 – 684 = 386 W/m^2)*, which is exactly identical to what has been recorded at the two principal-directions in summer.

Fig. (12) also shows that throughout the day there is only one time-period *(17:00-18:00)* in which $CCS_{(std)}$ receives more $I_{(HTCS)}$ than that received by flat roof. This scenario has not existed when the CCS*(std)* faced (N-S) in summer. The (NW-SE) orientation remains more preferable orientation for $CCS_{(std)}$ than facing (E-W), which created two undesirable times during the early-morning and the late-afternoon. In other words, during June and when $CCS_{(std)}$ faces (NW-SE), the desirable time period comparatively to (N-S), in which $CCS_{(std)}$ receives less $I_{(HTCS)}$ than flat roof, is shorter one hour, as it ends one hour earlier *(17:00 instead of 18:00)*.

$CCS_{(std)}$ Faces (NW-SE) During December

Fig. (13) shows the $I_{(HTCS)}$ on flat roof and curved roof $CCS_{(std)}$ during winter. It shows an exceptional scenario in which the maximum received solar radiation on curved roof $CCS_{(std)}$ shifts from midday unlike the flat roof behaviour.

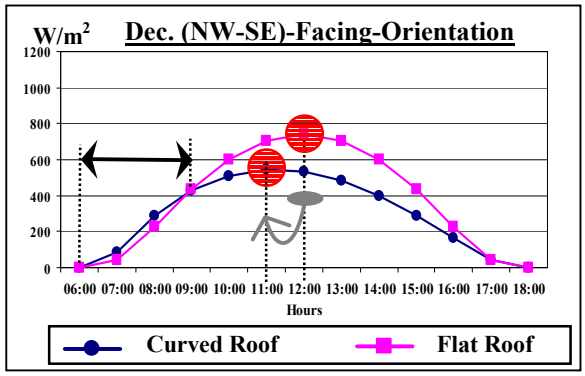

Fig. 13: $I_{(HTCS)}$ (W/m^2) on Flat Roof and $CCS_{(std)}$

This scenario is not similar to any previous principal-directions in summer or winter. Even more it is different than the first secondary-direction (NW-SE) in summer. Customary the maximum $I_{(HTCS)}$-value on flat roof is recorded at midday. Each $I_{(HTCS)}$-curve in both geometries ascends after 6:00 in the morning where both curves are still encountered.

Each $I_{(HTCS)}$-curve behaves differently during 7:00 and 8:00. $I_{(HTCS)}$-curves get very close again during the early-morning period at 9:00, in which $I_{(HTCS)}$-values are nearly equal, 430W/m^2 and 434 W/m^2 respectively, Fig.(13). Only after 6:00 and during the early-morning period $CCS_{(std)}$ receives notably more solar radiation than the flat roof.

On the contrary to what has been observed in summer, the noticeable difference has been delayed 3 hours in the winter morning *(from 6:00 to 9:00)*. As shown in Fig. (13), the difference between the two $\boldsymbol{I}_{(HTCS)}$-curves records its minimum around 9:00 in the morning and the late-afternoon hours *(17:00 &18:00)*. Dissimilar to all previous cases, the maximum difference is not recorded at the peak *(11:00 in this exceptional case)*. Moreover, this maximum difference takes place at 13:00 *(704– 483 = 221 W/m^2)*.

CCS$_{(std)}$ Curvature Faces Northeast & Southwest

This is the second secondary-orientation that the study employs. In this case, the longitudinal axis *(perpendicular on the CCS)* is the (NW-SE) axis. The two halves of CCS$_{(std)}$ face NE and SW. This case will be tested independently during summer and winter to clarify in which time of the year can curved roofs significantly reduce the received solar radiation than flat roofs.

CCS$_{(std)}$ Faces (NE-SW) During June

Fig. (14) shows $\boldsymbol{I}_{(HTCS)}$ of a flat roof and curved-roof CCS$_{(std)}$ during summer. This is an identically reversed scenario of the previous one (NW-SE) <u>*Refer to Fig. (12)*</u>, in which all features and analyses are inversed around the midday axis (12:00).

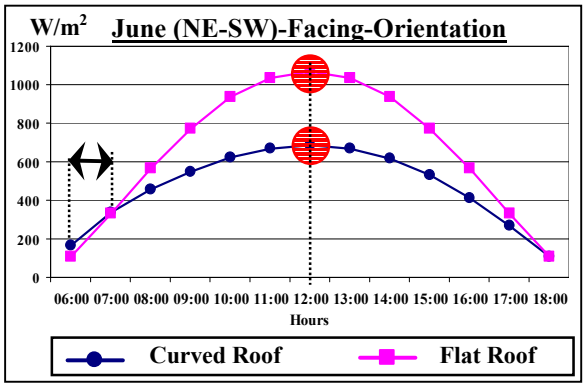

Fig. 14: $\boldsymbol{I}_{(HTCS)}$ (W/m^2) on Flat Roof and CCS$_{(std)}$

CCS$_{(std)}$ Faces (NE-SW) During December

Similarly to summer, the winter scenario of this secondary-facing-direction (NE-SW) is identically inversed of the first secondary-facing-direction (NW-SE) in winter, Fig. (15) <u>*Refer to Fig. (13).*</u>

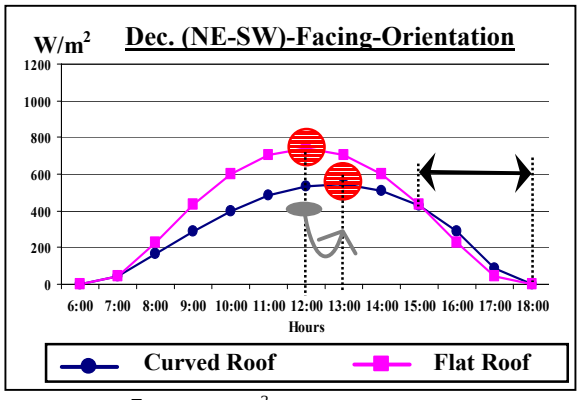

Fig. 15: $\boldsymbol{I}_{(HTCS)}$ (W/m^2) on Flat Roof and CCS$_{(std)}$

CONCLUSION

SMSR produced valuable predictions with accurate procedures calculating the total clear sky intensity of solar radiation on the semicircular curved roof (initial case CCS$_{(std)}$), in which CCSR always equals 1 *(A = B)*. At the same geographical latitude, ***SMSR*** results showed that the ratio between the received solar radiation amount W/m^2 by flat roof differs significantly from that received by sloped surfaces which resemble the form of a curved roof.

By testing the same CCSR at different orientations, the parametrical study and ***SMSR*** highlighted the magnitude of CCS orientation to control the received solar radiation intensity. It has been noticed that the calculated solar radiation amount on one planar segment varies significantly if either its slope angle or orientation has been slightly changed.

Principal Facing Directions

At all principal-directions, solar radiation readings, $\boldsymbol{I}_{(HTCS)}$-values, and consequently the resulted-difference due to the geometrical configurations are exactly identical around the midday axis. $\boldsymbol{I}_{(HTCS)}$-curves for any geometry are exactly symmetrical around the midday axis. In both summer and winter, regardless to the roof geometry, $\boldsymbol{I}_{(HTCS)}$-peaks are recorded at midday.

Despite of testing only one curvature *(invariable* CCSR *in this paper)*, it has been concluded that the generated drops in the $\boldsymbol{I}_{(HTCS)}$ values and distribution forms on the two tested roofs keep varying from case to another due to CCS$_{(std)}$ orientation and seasonal variation. But it is clearly noticed that $\boldsymbol{I}_{(HTCS)}$-curves and their shapes are always symmetrical around midday axis. Moreover, regardless of roof forms and relevant to the sun position at 12:00 in summer, which is almost perpendicular to geographical latitudes near the equator (23.58^{o}N) both principal-orientations generated identical $\boldsymbol{I}_{(HTCS)}$-values during midday.

On the other hand, in winter and due to the low position of the sun comparatively to summer, which means that the orientation is effectible as long as the tested geometry is not a flat roof. On the daily-average bases (N-S)-facing-orientation seems to be more energy-efficient in terms of making the $CCS_{(std)}$ receives 66.3% from that received on flat roof. Whereas, $CCS_{(std)}$ receives 75.4% from that has been received by the flat roof .

Secondary Facing Directions

Excluding the flat roof, $\boldsymbol{I}_{(HTCS)}$-values and other generated results are not identical around 12:00 in secondary-directions. $\boldsymbol{I}_{(HTCS)}$-curve for any geometry except the flat roof is NOT exactly symmetrical around the midday axis. Secondary-directions showed that throughout the year, both roofs geometries $\boldsymbol{I}_{(HTCS)}$-peaks are recorded at midday only during summer. Whereas, in winter only flat roof $\boldsymbol{I}_{(HTCS)}$-peak is recorded at 12:00, all other geometries' $\boldsymbol{I}_{(HTCS)}$-peaks are recorded variably at different hours either before or after 12:00.

Table (2) illustrates the percentages of day average received $\boldsymbol{I}_{(HTCS)}$ on different oriented $CCS_{(std)}$ relatively to flat roof during summer and winter. The table may help figuring out the preferable form and orientation for curved roof according to the geogaphical latitude and the desired solar intensity.

Table 2: Summer & Winter $\boldsymbol{I}_{(HTCS)}$ **%** *($CCS_{(std)}$ / Flat)*

Roof Geometry		Day Average $\boldsymbol{I}_{(HTCS)}$ W/m²		$\frac{I_{(HTCS)}\ CCS_{(std)}}{I_{(HTCS)}\ flat}$ %	
		June	Dec.	June	Dec.
Flat- Roof		**659**	**365**		
$CCS_{(std)}$	**N-S**	**437**	**304**	**65.85**	**83.28**
	E-W	**497**	**287**	**75.41**	**78.63**
	NW-SE	**469**	**290**	**71.16**	**79.45**
	NE-SW	**469**	**290**	**71.16**	**79.45**

ACKNOWLEDGMENT

I would like to thank The Arab Academy For Science and Technology www.aast.edu for their financial support for this research project. I would like also to thank my supervisor Dr. M. B. GADI for his countinued support and assistance with my research project and throghout the parametrical study and results interptations.

REFERENCES

Archnet Digital Library. Internet WWW Page at: www.archnet.org

Elseargy A. B. & Gadi M. B., Roofs Geometric Forms and Solar Irradiation Intensity In Hot-arid Climates, ISES Solar World Congress, ISES2003, Gothenburg, Sweden, 14-19 June 2003.

Laouadi A. & Atif M. R., Prediction models of optical characteristics for domed skylights under Standard and Real Sky Conditions, Institute of Research in Construction, National Research Council Canada, NRC-CNRC, 7th International IBPS Conference Rio de Janeiro, Brazil, August 13-15, 2001.

Laouadi A. & Atif M. R., Transparent domed skylights: *Optical model for Predicting Transmittance, Absorptance and Reflectance*, Institute of Research in Construction, National Research Council Canada, NRC-CNRC

Solar Radiation Simulation Model ***SRSM***. Internet WWW Page at: www.jgsee.kmutt.ac.th/exell/Solar/SolradJS.htm

Stasinopoulos T. N., Form Insolation Form Index; n*otes on the relation of geometric shape and solar irradiation*, Environmentally Friendly Cities - *Proceedings of PLEA 98 Passive and Low Energy Architecture, Lisbon, Portugal, June 1998.*

Stasinopoulos T. N., Geometric Forms & Insolation; *An analytical Study of the Influence of Shape on Solar Irradiation*, Doctoral Dissertation – Dept. of Architecture - National Technical University of Athens, Athens, March 1999.